

STRESS Counting Supernovae

Maria Teresa Botticella¹
 Enrico Cappellaro²
 Marco Riello³
 Laura Greggio²
 Stefano Benetti²
 Ferdinando Patat⁶
 Massimo Turatto⁵
 Giuseppe Altavilla⁴
 Andrea Pastorello¹
 Stefano Valenti¹
 Luca Zampieri²
 Avik Harutyunyan⁷
 Giuliano Pignata⁸
 Stefan Taubenberger⁹

¹ Queen's University Belfast, UK

² INAF–Osservatorio Astronomico di Padova, Italy

³ Institute of Astronomy, Cambridge, UK

⁴ INAF–Osservatorio Astronomico di Bologna, Italy

⁵ INAF–Osservatorio Astronomico di Catania, Italy

⁶ ESO

⁷ INAF–Fundación Galileo Galilei, Canary Islands, Spain

⁸ Departamento de Astronomia, Universidad de Chile, Chile

⁹ Max-Planck-Institut für Astrophysik, Garching, Germany

The rate of occurrence of supernovae (SNe) is linked to some of the basic ingredients of galaxy evolution, such as the star formation rate, the chemical enrichment and feedback processes. SN rates at intermediate redshift and their dependence on specific galaxy properties have been investigated in the Southern Intermediate Redshift ESO Supernova Search (STRESS). The rate of core collapse SNe (CC SNe) at a redshift of around 0.25 is found to be a factor two higher than the local value, whereas the SNe Ia rate remains almost constant. SN rates in red and blue galaxies were also measured and it was found that the SNe Ia rate seems to be constant in galaxies of different colour, whereas the CC SN rate seems to peak in blue galaxies, as in the local Universe.

Why count SNe?

A complete and coherent picture of the formation and evolution of galaxies is a fundamental objective of observational astronomy. Star formation (SF) is one of the main processes driving the evolution of galaxies. Individual young stars are unresolved in almost all nearby galaxies even with the Hubble Space Telescope, but the integrated luminosity in the ultraviolet (UV) continuum, nebular emission lines such as H α or [O II] and the infrared (IR) continuum provides a direct, sensitive probe of these young massive star populations in the galaxies. Integrated light measurements in these wavelength ranges scale linearly with the current star formation rate (SFR) and are used to investigate the SF properties of galaxies. An alternative and complementary approach to trace the SFR is based on direct observation of the death of some stars through SNe.

There are two distinct types of explosion: core-collapse-induced explosion of short-lived massive stars (CC SNe) and thermonuclear explosion of long-lived low mass stars (SNe Ia). Stellar evolution theory predicts that all stars more massive than eight to ten solar masses complete their nuclear burning and develop an iron core that cannot be supported by any further nuclear fusion reactions, or by electron degenerate pressure. The subsequent collapse of the iron core results in the formation of a compact object, a neutron star or a black hole, accompanied by the high velocity ejection of a large fraction of the progenitor mass. Due to the short lifetime of progenitor stars (from a few tenths of a million to several tens of millions of years), the CC SN rate is directly proportional to the current SFR. Poor statistics is a major limiting factor for using the CC SN rate as a tracer of the SFR both at low redshift, due to the difficulty of sampling large volumes, and at high redshift, due to the difficulty of detecting and typing faint SNe. Moreover a significant fraction of CC SNe are missed by SN searches, since they are embedded in dusty spiral arms or galactic nuclei, and this fraction may change with redshift, if the amount and the average properties of dust in galaxies evolve with time. As a consequence an appropriate correction is required to estimate the intrinsic SN rate from the number of discovered CC SNe.

SNe Ia are widely believed to originate from the thermonuclear explosion of a carbon and oxygen white dwarf (WD) in a binary system, but the nature and evolution of the binary system remain poorly constrained. Progenitor models are broadly classified as either: single degenerate (SD) in which a WD, accreting from a main sequence or red giant companion, grows in mass until it reaches a critical limit and explodes; or double degenerate (DD), in which a close double WD system merges after orbital shrinking due to the emission of gravitational wave radiation. The time elapsed from the birth of the binary system to the SN explosion (delay-time) spans a wide range, from tens of millions of years to ten billion years or more. As a consequence the SN Ia rate reflects the star formation history (SFH) of a galaxy according to the distribution of the delay times.

SNe Ia can act as standard candles due to their significant intrinsic brightness, ubiquity and homogeneity, and have provided the first evidence for an acceleration of the expansion of the Universe. Understanding the mechanism that is responsible for this accelerating expansion, i.e., the nature and amount of dark energy, is one of the crucial next steps for observational cosmology and requires new searches for SNe Ia. Given the importance of SNe Ia as cosmological probes, the questions whether SNe Ia are a homogeneous class of stellar explosion and whether their properties evolve with redshift require answers. In particular the investigation of the nature of the progenitor star has become a critical issue. The analysis of the SN Ia rate as a function of redshift, galaxy morphological type and colour is a powerful tool for investigating the nature of the progenitor stars, their possible evolution with redshift and their connection with the environment.

Why STRESS?

Progress in using the CC SN rate as a SFR tracer and in investigating the nature of SN Ia progenitors requires accurate measurements of SN rates at various cosmic epochs. To reduce the uncertainty in the estimates of SN rates, a statistically significant SN sample and strict control of systematic effects, in particular

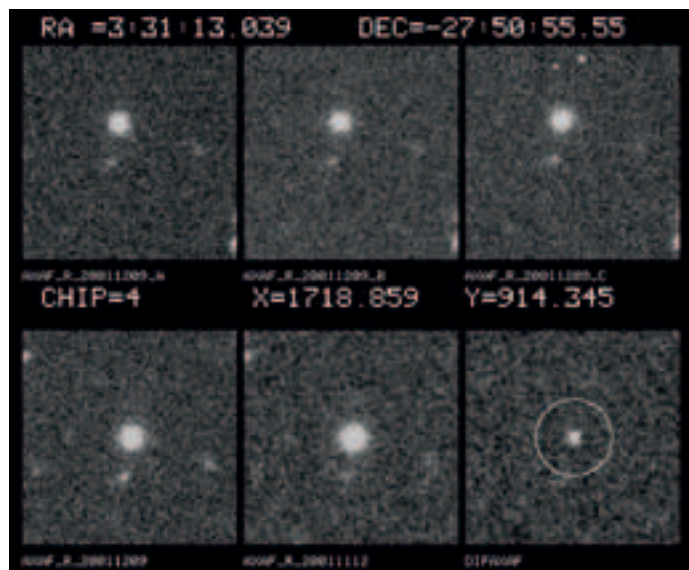


Figure 1. An example of a SN candidate discovered in the *R*-band. At the top are images of the same sky field acquired with a small offset of the telescope pointing (jittered images). These images are acquired to allow a better removal of cosmetic defects, cosmic rays, satellite tracks and fast moving objects. At the bottom left and centre are two images acquired at different epochs (obtained stacking the jittered images), with the difference image to the right. The variable source appears projected on a galaxy and shows a point-source-like profile in the difference image.

concerning dust attenuation, are necessary. Since SNe are rare and transient events, deep observations of a large sky field with a suitable time interval are required to maximise the number of SNe discovered. Early SN searches based on visual observations of nearby galaxies or photographic surveys with Schmidt telescopes were confined to the local Universe. Collecting data from five nearby SN searches (137 discovered SNe) and adopting an empirical correction for dust attenuation, based on the morphological type and inclination of SN host galaxies, it has been possible to estimate the SN rates in the local Universe as a function of both galaxy morphological type and colours (Cappellaro et al., 1999).

Nowadays, by using panoramic detector arrays mounted on medium-size telescopes, it has become possible to monitor large sky fields and to sample an adequate volume of the Universe with a reasonable amount of telescope time. The Wide Field Imager (WFI), a mosaic camera consisting of eight CCDs with a field

of view of 0.5 square degrees mounted at the 2.2 m MPG/ESO telescope, is an excellent example of this type of instrumental setup. New technological capabilities have allowed the SN sample to be greatly enlarged, leading to the discovery of SNe up to redshifts greater than one. Despite this progress, measurements of SN rates are still scant (in particular for CC SNe) and uncertain (for both SN types). The main goal of almost all SN surveys performed in the last few years has been to investigate the expansion of the Universe and the properties of the dark energy using SNe Ia as standard candles. The observing strategy of these searches was tuned to identify *bona fide* SN Ia candidates before maximum light and confirm spectroscopic type only for these candidates. As a consequence the SN sample collected by these surveys is seriously incomplete, so that the measurement of the rate for SNe Ia is troublesome and for CC SNe nearly impossible.

STRESS was devised to improve SN rate determinations (Botticella et al., 2008). The observing strategy was specifically designed to measure both CC SN and SN Ia rates at intermediate redshift, and the SN detection and classification processes were tuned to collect an unbiased and homogeneous sample of both SN types. In addition, we aimed to investigate the evolution of SN rates by comparing our estimates with those obtained in the local Universe and to relate the SN events to SF in the parent galaxies by



Figure 2. An example of a SNorAGN candidate discovered in the *V*-band (layout of images as in Figure 1). The variable source occurs near the galaxy nucleus. This candidate is actually an AGN and was also discovered by the Sloan Digital Sky Survey.

collecting detailed information on the galaxy sample including their photometric properties and dust content. In order to preserve the link between SNe and their parent galaxies, we measured SN rates by counting the events discovered in a selected galaxy sample, rather than those detected in a given volume. This approach involved the following steps: the selection of the galaxy sample and its characterisation; the detection and classification of SN candidates; the measurement of SN rates; the analysis of their dependence on the colour of the host galaxy; and their evolution with redshift.

How to handle STRESS

STRESS is a multi-year project (from 2000 to 2005) consisting of two related observing programmes: an imaging programme, intended both to search for SN candidates and to obtain colour information for the monitored galaxies, and a spectroscopic programme to type SN candidates and measure their redshift. The imaging programme was carried out with the 2.2 m MPG/ESO telescope equipped with WFI in the *V*-band over the first four years (Cappellaro et al., 2005), and in the *R*-band, targeting SNe at higher redshifts in the last year (Botticella

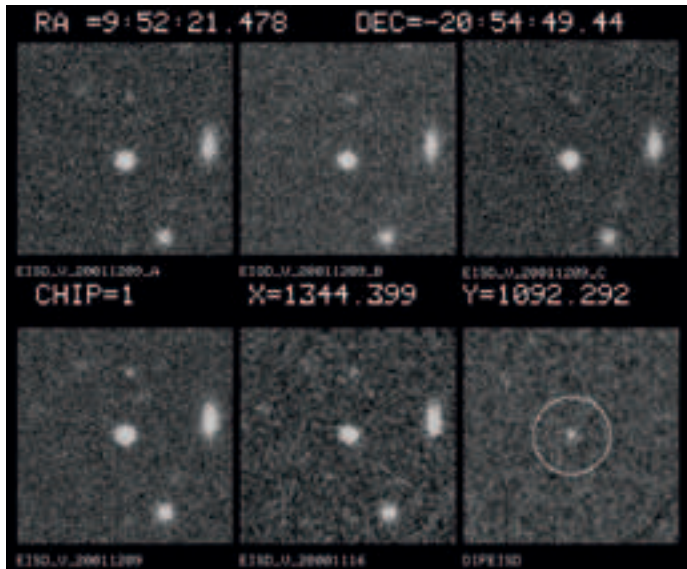


Figure 3. An example of a variable star discovered in the V-band (layout of images as in Figure 1). The source shows a stellar profile on all images.

et al., 2008). Spectra were acquired with the Very Large Telescope (VLT) equipped with the FOcal Reducer and low dispersion Spectrograph (FORS1 and FORS2). Sixteen sky fields were imaged on average once every four months and spectroscopic observations were scheduled about one week after imaging observations to secure SN candidate typing.

SN candidates were identified by subtracting images acquired at different epochs using the Optimal Image Subtraction code (OIS) in the Alard (2000) package. The resulting image was searched for variable sources (SN candidates — Figure 1; variable Active Galactic Nuclei (AGNs) — Figure 2; variable stars — Figure 3; and asteroids — Figure 4) using a source detection code (SExtractor, Bertin & Arnouts, 1996). There were often spurious sources on the difference images due to imperfect removal of bright stars, cosmic rays and hot or dead CCD pixels. To reject these artefacts and to obtain a first classification of actual variable sources we used a custom-made ranking program that assigns a score to each source based on several parameters (magnitude, shape, position) measured by SExtractor. The score was tuned using a training dataset of known events and extensive simulations. The final selection of *bona fide* SN candidates, about ten per image, was made by visual

inspection. We classified as SN candidates those sources with a stellar profile in the difference image that appeared projected on a galaxy (see Figure 1), and as SNorAGN candidates all those sources detected within a radius of 0.5 arcsec from the host galaxy nucleus (Figure 2).

We developed a database of information about each detected variable source with a search engine to identify independent detections of the same source at different epochs and in different filters. SN and SNorAGN candidates were cross-checked with all sources in the database before spectroscopic typing. This allowed us to clear the SNorAGN sample, identifying AGNs by their long-term, irregular variability.

Spectroscopic observations were planned for all SN candidates and the remaining SNorAGN, but we could classify only 40% of the candidates because of limited telescope time allocation. At the end of STRESS we re-analysed all variable sources in the database to obtain a final classification. We also carried out a new spectroscopic programme using FORS2 to obtain the redshift and to check for signs of the presence of AGN in the host galaxies of those candidates without spectroscopic typing. Combining information from the long-term variability, direct and host galaxy spectroscopy, we found that 50% of the variable sources originally classified as SNorAGN were actually AGN. Our final SN sample consists of 25 SNe

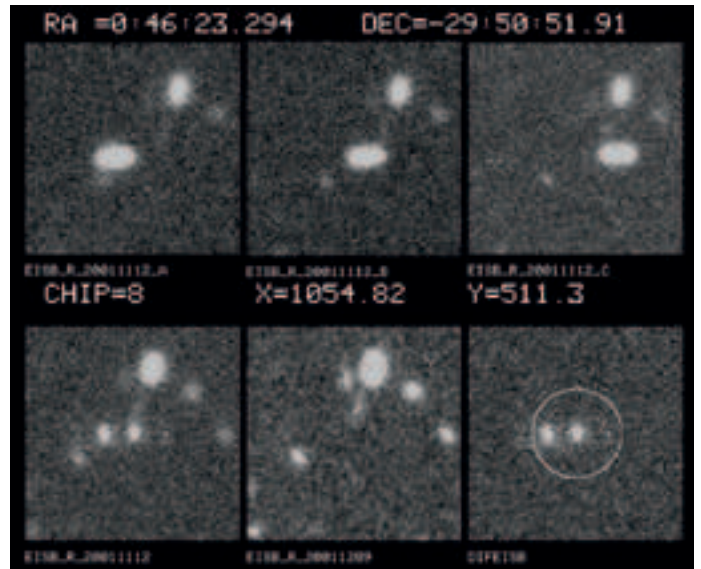


Figure 4. An example of an asteroid discovered in the R-band (layout of images as Figure 1). The source shows up at a different position on the jittered images and thus as an irregular shape in the stacked image. No source was visible in the image acquired one month before.

(9 SNe Ia and 16 CC SNe), 33 SN candidates and 28 SNorAGN candidates.

For the selection of the galaxy sample and the measurement of galaxy properties (colours, redshift, absolute luminosity) we used multi-band (*BVRi*) images obtained during the SN search programme. To produce a catalogue of the monitored galaxies we selected all images with the best seeing and sky transparency for each field and band, stacked them, detected all sources on the resulting deep images and selected galaxies (43283 in total) using the SExtractor classifier. The galaxy colours have been estimated by measuring flux in the same physical region (adaptively scaled to the galaxy dimensions) in all bands. The galaxy redshift and the absolute *B*-band luminosity were obtained by comparing observed and predicted galaxy colours as a function of redshift with a spectral energy distribution template fitting technique.

The results of STRESS

Three basic ingredients are required to estimate the SN rate in a galaxy sample: the number and type of SNe discovered; the time of effective surveillance of the

sample in order to relate the detection frequency to the intrinsic SN rate (control time); and a physical parameter, proportional to the stellar content of each galaxy, to normalise the rate.

The control time is defined as the time during which a SN occurring in a given galaxy can be detected by the search, and depends on the shape of the SN light curve, distance and dust extinction of the galaxy, instrumental setup, observing strategy and detection technique of the SN search. The effect of dust attenuation on the control time has been estimated by modelling SN and dust distributions in galaxies. In short, following the method described in Riello & Patat (2005), we performed Monte Carlo simulations where artificial SNe were generated with a predefined spatial distribution function, and were viewed from random lines of sight. Integrating the dust column density along the line of sight for each SN, we derived the total optical depth and the relative attenuation. Repeating a number of simulations, we obtained the expected distribution of SN absorption. We considered three possible scenarios for the amount of dust in a galaxy assuming different total optical depths along the galaxy rotation axis ($\tau = 0$ — no extinction, $\tau = 1$ — standard extinction, $\tau = 5$ — high extinction). For CC SNe the control time was estimated for each extinction scenario. For SNe Ia we did not consider the high extinction scenario, since it is expected to occur, on average, in environments with a smaller amount of dust. Monte Carlo simulations also allowed us to probe the most relevant parameters affecting the SN detection efficiency. In each simulation, artificial SNe of different magnitudes were added to an image that was then searched for variable sources using the same software as in the actual search. The detection efficiency at a given magnitude was computed as the ratio between the number of discovered and injected artificial sources.

The normalisation parameter for SN rates can be the galaxy mass or a mass tracer, e.g., the blue luminosity, in which case the rate is expressed in SN per unit galaxy mass ($\text{SNuM} = 1\text{SN}/10^{10} M_B/\text{century}$), or in terms of galaxy luminosity ($\text{SNu} = 1\text{SN}/10^{10} L_B/\text{century}$), respectively. Since the estimate of the galaxy mass

is uncertain (and makes use of the galaxy luminosity as a mass tracer anyway), we chose to determine the rate in SNU.

The SN rate at a given redshift is computed as the ratio between the number of discovered SNe and the control time of the monitored galaxies at the given redshift. Since our SN sample spans a wide redshift range (0.06–0.6), we can obtain some constraints on the evolution of the rate. We adopted a power law parameterisation for the redshift dependence of the SN rate with two free parameters: the rate at the weighted average of the galaxy redshifts, with weights given by the respective control time; and an evolution index. The best-fit values of the free parameters were obtained by comparing the observed SN redshift distribution with the expected one.

Our results indicate that the SN Ia rate appears almost constant up to redshift $z = 0.3$, whereas the SN CC rate has already increased by a factor of two by redshift $z = 0.2$. The different evolutionary behaviour of CC SN and SN Ia rates implies that their ratio increases by a factor of two from the local Universe to redshift $z = 0.25$ (about three billion years ago), thereby requiring that a significant fraction of SN Ia progenitors have a lifetime longer than three billion years. The estimate of the SN rate evolution depends on the correction applied for dust extinction. For instance, the ratio between the CC SN rate at redshift $z = 0.2$ and that in the local Universe varies from 1.6 to 2.8, depending whether a no extinction or a high extinction scenario is assumed. However, the fact that the CC SN rate increases faster than the SN Ia rate appears to be a robust result.

We also investigated the dependence of SN rates on galaxy colour, an indicator of the stellar population and SFR. We split our galaxy sample and the local galaxy sample by Cappellaro et al. (1999) into blue and red sub samples, according to the observed $B-V$ colour and adopting the rest frame $B-V$ colour of an Sa galaxy ($B-V = 0.45$) as a reference. The SN Ia rate appears almost constant in galaxies with different $B-V$ colour, whereas the CC SN rate strongly increases from red to blue galaxies, both at redshift $z = 0.25$ and in the local Universe.

Finally we compared the observed evolution of SN rates with the behaviour predicted by the cosmic SFH, assuming various SN progenitor models and different extinction scenarios. This comparison provides interesting clues about the reliability of SN progenitor models and the adequacy of the dust extinction correction of SN rates. We collected published measurements of SN rates at intermediate and high redshifts that are in units of co-moving volume. To convert our measurements from SNU to volumetric units, we multiplied the rates by the total blue luminosity density at the redshift of our estimated rates. Since the blue luminosity density increases with redshift, the volumetric SN rates evolve faster than the rates in SNU. We found an increase of a factor two at redshift $z = 0.3$ for SNe Ia, and a factor of about three at redshift $z = 0.2$ for CC SNe (see Figures 5 and 6).

The CC SN rate expected for a given SFH depends on the mass range of the progenitors, on the initial mass function (IMF) describing the distribution of the stellar masses and on the correction due to dust extinction. We assumed that the mass of CC SN progenitors ranges from 8 to $50 M_{\odot}$ and that the IMF has a Salpeter slope, with a turnover below 0.5 solar masses. Since there is a large scatter between the measurements obtained with different SFR indicators, it is difficult to obtain a consistent picture of the SFH. We selected two representative prescriptions for the SFH in the literature: the piecewise linear fit of SFR measurements from different tracers (Hopkins & Beacom, 2006) and the linear fit to the SFR measurements from the $H\alpha$ emission line (Hippelstein et al., 2003). The measurements of CC SN rate confirm the steep increase with redshift expected with both SFHs (Figure 5). The evolution predicted from the SFH based on $H\alpha$ fits the CC SN rate measurements very well, while the SFH by Hopkins & Beacom requires higher CC SN rates both in the local Universe and at high redshift.

If we correct our measurements and the local CC SN rate measurements according to the high extinction scenario, we obtain an acceptable agreement between the data and the predictions of the Hopkins & Beacom SFH. However, this correction requires an extremely high

dust content in galaxies, which needs to be confirmed with new accurate measurements in nearby and distant galaxies, and also requires a better estimate of the fraction of obscured CC SNe that are missed in optical SN searches.

Alternatively we may consider the possibility of a narrower range for the CC SN progenitor masses: in particular, a lower limit of 10–12 M_{\odot} would bring the observed CC SN rates into agreement with the SFH by Hopkins & Beacom. On the other hand, estimates of the progenitor mass from the detections of stars in pre-explosion images seem to favour a lower limit of about 8–10 M_{\odot} (Smartt et al., 2008). This result illustrates that it is necessary to reduce the uncertainties in the cosmic SFH and to apply a consistent dust extinction correction both to SF and to CC SN rates in order to constrain the mass range of CC SN progenitors. A comparison of the CC SN rate with other SFR tracers in the same galaxy sample could shed light on these issues.

The cosmic evolution of the SN Ia rate is modulated by two critical ingredients: the SFH and the delay time distribution (DTD). Different SFHs give different evolutionary paths (Blanc & Greggio, 2008), but we have considered only the SFH by Hopkins & Beacom. We estimated the evolution of SN Ia rate by convolving this SFH with different formulations of the DTD: three distributions related to different SN Ia progenitor models and described by the analytical formulation of Greggio (2005); the parameterisation by Mannucci et al. (2006), designed to address some specific observational constraints, regardless of the correspondence with a specific progenitor scenario. All DTDs appear to predict a SN Ia rate evolution consistent with the observations, with the exception of the ‘wide’ DD model, which appears too flat (see Figure 6). At the same time, with the adopted SFH none of the explored DTD functions are able to reproduce both the rapid increase from redshift $z = 0$ to $z = 0.5$ and the decline at redshift greater than one, suggested by some measurements. With the current data on the rate evolution, it is difficult to discriminate first between different DTDs and then between different SN Ia progenitor

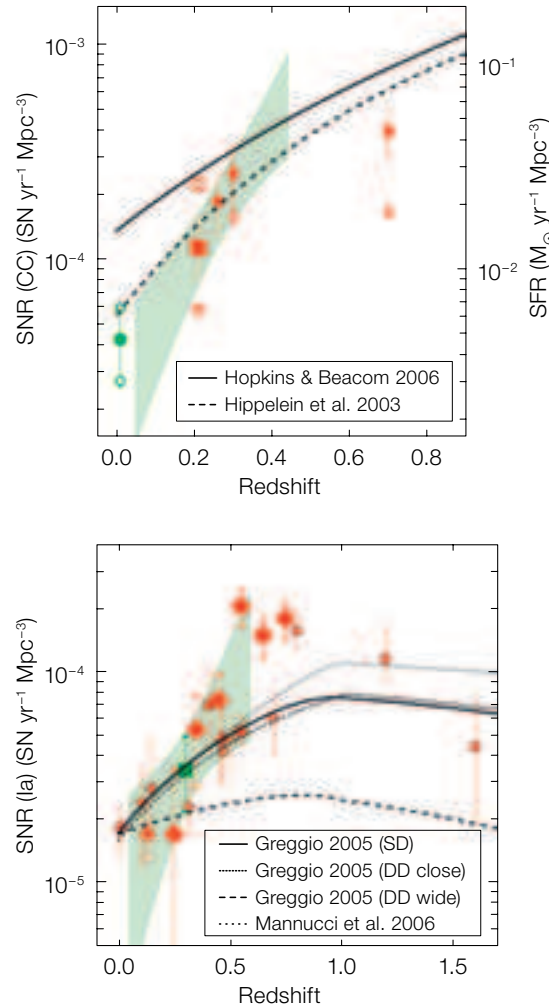


Figure 5. Comparison between the core collapse (CC) SN and the SF rate evolution. Lines are selected star formation histories from the literature. The shaded area represents the 1σ confidence level of our estimate of CC SN rate evolution as deduced from the likelihood fit. Circles show local measurements by Cappellaro et al. (1999); squares are measurements by Botticella et al. (2008); the pentagon is the measurement by Cappellaro et al. (2005), and the rhombi the measurements by Dalhen et al. (2004). Filled symbols are measurements obtained assuming a standard extinction correction. The lower open symbols are measurements not corrected for extinction while the upper open symbols are measurements obtained adopting a high extinction correction.

Figure 6. SN Ia rate measurements in the literature and predictions obtained by convolving the SFH of Hopkins & Beacom with various delay time distribution functions. The predicted paths are plotted as lines with different types (see inset box for key). The shaded area represents the 1σ confidence level of our estimate of SN Ia rate evolution as deduced from the likelihood fit. The circle is the measurement of Cappellaro et al. (1999); the inverted triangle from Madgwick et al. (2003); the leftward triangle for Hardin et al. (2000); the triangle for Blanc et al. (2004); the rightward triangles for Neill et al. (2007); the green square for Botticella et al. (2008); the rhombi for Barris & Tonry (2006); the small rhombus for Tonry et al. (2003); the pentagon for Neill et al. (2006); the red square from Pain et al. (2002); and the hexagons for Dahlen et al. (2004).

models. Measurements of the SN Ia rate in star-forming and passively evolving galaxies over a wide range of redshifts can provide more significant evidence about the progenitor models.

the lack of spectroscopic classification of SN candidates.

Future wide-field SN surveys at ESO telescopes, such as SUDARE on the VLT Survey Telescope (VST) equipped with OmegaCam, will be able to discover thousands of SNe and will enable accurate measurements of the SN rates, providing an unbiased census of the host galaxies. A different observing strategy that consists of the frequent, long-term monitoring of a few selected sky fields (rolling search), will allow us to detect SN candidates and obtain their light curves in different bands at the same time. Photometric typing, based on the shape of the light curve and colour evolution, for all SN candidates will reduce the uncertainty due to

References

Alard, C. 2000, *A&A*, 144, 363
 Barris, B. J. & Tonry, J. L. 2006, *ApJ*, 637, 427
 Bertin, E. & Arnouts, S. 1996, *A&A*, 117, 393
 Blanc, G. & Greggio, L. 2008, *New A.*, 13, 606
 Botticella, M. T. et al. 2008, *A&A*, 479, 49
 Cappellaro, E. et al. 1999, *A&A*, 351, 459
 Cappellaro, E. et al. 2005, *A&A*, 430, 83
 Dahlen, T. et al. 2004, *ApJ*, 613, 189
 Greggio, L. 2005, *A&A*, 441, 1055
 Hardin, D. et al. 2000, *ApJ*, 613, 189
 Hopkins, A. M. & Beacom, J. F. 2006, *ApJ*, 651, 142
 Hippelein et al. 2003, *A&A*, 402, 65
 Madgwick, D. et al. 2003, *ApJ*, 599, L33
 Mannucci et al. 2006, *MNRAS*, 370, 773
 Neill, J. D. et al. 2006, *ApJ*, 132, 1126
 Neill, J. D. et al. 2007, *ApJ*, 661, 123
 Pain, R. et al. 2002, *ApJ*, 577, 120
 Riello, M. & Patat F. 2005, *MNRAS*, 362, 671
 Smartt, S. et al. 2008, arXiv:0809.0403
 Tonry, J. L. et al. 2003, *ApJ*, 594, 1